

## Identification of the cadmium vacancy in CdTe by electron paramagnetic resonance

P. Emanuelsson and P. Omling

*Department of Solid State Physics, University of Lund, Box 118, S-221 00 Lund, Sweden*

B. K. Meyer

*Physikdepartment E16, Technical University of Munich, D-8046 Garching, Federal Republic of Germany*

M. Wienecke and M. Schenk

*Institute of Crystallography and Materials Research, Department of Physics, Humboldt-University of Berlin, Invalidenstrasse 110, D-1040 Berlin, Federal Republic of Germany*

(Received 11 January 1993)

The isolated cadmium vacancy in CdTe is identified by means of electron paramagnetic resonance (EPR) in its single negative charge state. The spectrum reveals that the defect has trigonal symmetry, which can be explained in a model in which the hole occupies a dangling-bond  $t_2$  orbital, and the orbital degeneracy is removed by a Jahn-Teller distortion. From the hyperfine interaction it is concluded that the hole is highly localized on one of the four tellurium neighbors. Photo-EPR measurements indicate that the  $2-/-$  acceptor level is situated less than 0.47 eV above the valence band.

### I. INTRODUCTION

The cation vacancy in II-VI compounds introduces a double acceptor level in the forbidden energy gap, and this defect has been identified by means of electron paramagnetic resonance (EPR) in BeO,<sup>1</sup> ZnO,<sup>2</sup> ZnS,<sup>3,4</sup> ZnSe,<sup>3,5</sup> and CdS.<sup>6</sup> In all these systems the spectrum of the negatively charged metal vacancy was found, and the spin was determined to be  $\frac{1}{2}$ . In ZnO, an additional spectrum with spin  $S=1$  corresponding to the neutral zinc vacancy was observed.

In the crystals with zinc-blende structure (ZnS and ZnSe), the symmetry of the defect was found to be  $C_{3v}$  ( $3m$ ). This deviation from  $T_d$  ( $43m$ ) symmetry was explained in a model in which the hole occupies a  $t_2$  orbital of the tellurium dangling bonds, and, because of the orbital degeneracy, the system is unstable to a static Jahn-Teller distortion.<sup>3,5</sup>

Lee and co-workers have performed optically detected magnetic-resonance (ODMR) measurements on luminescence bands observed in irradiated ZnS and ZnSe. They could show that the luminescence band centered at 720 nm in ZnSe and at 570 nm in ZnS corresponds to recombination processes from a shallow donor to the Zn vacancy acceptor.<sup>7-9</sup> From the dependence of the ODMR signals on the excitation and emission spectra, and using a configuration coordinate model, they could determine that the double acceptor level is located at  $E_v + 0.66$  eV in ZnSe and at  $E_v + 1.1$  eV in ZnS.

CdTe is one of the most promising II-VI compounds for device applications. It has a band gap of 1.6 eV which makes CdTe quantum wells with ZnTe as barrier material attractive for optoelectronic applications in the 1.6–2.4-eV range. It is also a suitable material for, for instance, nuclear radiation detectors and as substrate for  $Cd_xHg_{1-x}$ Te infrared detectors. Because of this, a great

deal of research has been performed on defects related to vacancies in CdTe.  $A$  centers, which consist of a metal vacancy and a nearby donor, have been investigated using EPR,<sup>10</sup> as well as ODMR,<sup>11,12</sup> and recently the Te vacancy was identified.<sup>13</sup>

In this paper we report the EPR identification of the isolated cation vacancy in CdTe, and we show that it is very similar to the Zn vacancy in ZnSe and ZnS.

### II. EXPERIMENTAL DETAILS

The sample used was a CdTe single crystal grown by the vertical Bridgman technique. The Cd and Te used for synthesizing the material were purified by multiple distillation and multiple zone refining, respectively. The as-grown material was  $p$ -type and had a carrier concentration of  $p \approx 8 \times 10^{14} \text{ cm}^{-3}$ . The crystal slices were annealed according to the three-phase equilibrium in a Te-rich atmosphere at 750°C for five days. At 750°C and under equilibrium conditions the carrier concentration was  $p = 1.2 \times 10^{17} \text{ cm}^{-3}$ .<sup>14</sup>

The EPR measurements were performed using a Bruker ESP 300 spectrometer equipped with a helium flow cryostat (Air Products) capable of controlling the temperature over the range from that of liquid helium to room temperature. The sample could be illuminated *in situ* with monochromatic light from a halogen lamp attached to a monochromator (Applied Photophysics F 3.4).

### III. RESULTS AND DISCUSSION

At temperatures around 25 K an EPR spectrum revealing trigonal symmetry was observed. In analogy with ZnSe and ZnS,<sup>3,5</sup> the spectrum is tentatively suggested to be caused by the  $V_{\text{Cd}}^-$  center. In the model proposed by Watkins for metal vacancy, the molecular orbitals of the center are linear combinations of the dangling-bond or-

bitals of the neighboring tellurium atoms.<sup>3</sup> For the doubly negatively charged vacancy, these orbitals,  $a_1$  and  $t_2$ , are completely filled and the configuration is  $a_1^2 t_2^6$  resulting in a  $^1A_1$  many-electron state. In the singly negatively charged state, one electron is missing, i.e., the configuration is either  $a_1^2 t_2^5$ , resulting in a  $^2T_2$  state, or  $a_1^1 t_2^6$ , resulting in a  $^2A_1$  state. The  $^2T_2$  state, which turns out to be the ground state, is orbital degenerate and is therefore unstable to a static Jahn-Teller distortion. In this case the distortion is found to be trigonal and the  $^2T_2$  state is split into a  $^2A_1$  and a  $^2E$  state with the  $^2A_1$  state lowest in energy. The energy-level scheme of the  $V_{Cd}^-$  center is shown in Fig. 1.

In the  $^2A_1$  ground state of  $V_{Cd}^-$  the hole is highly localized on one of the tellurium neighbors. The main feature of the hyperfine structure is therefore determined by the interaction with one Te nucleus. Tellurium consists to 92.1% of isotopes with nuclear spin  $I=0$ , and to 0.9% of  $Te^{123}$  and 7.0% of  $Te^{125}$  which both have  $I=\frac{1}{2}$ . The hyperfine structure should therefore consist of a strong central line (92.1% of the intensity) and two pairs of satellite lines (0.9% and 7.0% of the intensity for the two pairs, respectively). In addition, each line is split by the ligand hyperfine interaction with the three Cd neighbors of the Te atom. Cadmium consists to 75.0% of isotopes with  $I=0$ , and to 12.8% of  $Cd^{111}$  ( $I=\frac{1}{2}$ ) and 12.2% of  $Cd^{113}$  ( $I=\frac{1}{2}$ ). Since the gyromagnetic ratio is almost the same for  $Cd^{111}$  and  $Cd^{113}$ , no difference in the hyperfine interaction is expected to be observed between these two isotopes. Each EPR line is split by the ligand hyperfine interaction into a number of components depending on the number of Cd neighbors with  $I=\frac{1}{2}$ . In Fig. 2 (top) the EPR spectrum with the magnetic field parallel to the trigonal axis is shown. The hyperfine splitting caused by  $Te^{125}$ , as well as the ligand hyperfine splitting from the three neighboring Cd atoms, are clearly seen. The splitting due to  $Te^{123}$ , with an abundance of 0.9%, is not observable because of too low a signal-to-noise ratio.

The spin Hamiltonian for the defect, including the Zeeman, hyperfine, and ligand hyperfine interaction, can be written as

$$H = \mu_B \mathbf{B} \cdot \vec{g} \cdot \mathbf{S} + \mathbf{S} \cdot \vec{A}^{Te} \cdot \mathbf{I}^{Te} + \sum_j \mathbf{S} \cdot \vec{A}_j^{Cd} \cdot \mathbf{I}_j^{Cd}, \quad (1)$$

where all symbols have their usual meaning. If we neglect the ligand hyperfine interactions from the Cd neighbors, the energy of the level with magnetic quantum number of the electron spin  $M$  and magnetic quantum number of the nuclear spin  $m$  can be written as

$$E = g\mu_B BM + K^{Te} Mm. \quad (2)$$

Here,  $g$  and  $K^{Te}$  are determined by

$$g = [(g_{\parallel} \cos\theta)^2 + (g_{\perp} \sin\theta)^2]^{1/2}, \quad (3)$$

$$K^{Te} = [(g_{\parallel} A_{\parallel}^{Te} \cos\theta)^2 + (g_{\perp} A_{\perp}^{Te} \sin\theta)^2]^{1/2} / g, \quad (4)$$

where  $\theta$  is the angle between the trigonal axis and the applied magnetic field. By analyzing the angular dependence of the EPR spectrum with Eqs. (2)–(4), the spin Hamiltonian parameters could be determined to be  $g_{\parallel} = 1.955 \pm 0.001$ ,  $g_{\perp} = 2.143 \pm 0.001$ ,  $A_{\parallel}^{Te} = (56 \pm 3) \times 10^{-4} \text{ cm}^{-1}$ , and  $A_{\perp}^{Te} = (173 \pm 3) \times 10^{-4} \text{ cm}^{-1}$  (the values  $A_{\parallel}^{Te}$  and  $A_{\perp}^{Te}$  are given for the  $Te^{125}$  isotope). Because the three Cd neighbors form different angles between the Cd-Te bonds and the magnetic field, the ligand hyperfine structure from the different neighbors overlaps and for most directions of the magnetic field this structure could not be resolved. It was therefore not possible to determine the ligand hyperfine parameters. However, with the magnetic field parallel to the trigonal axis, all three angles between the “Cd neighbor bonds” and the magnetic field are the same and, therefore, the ligand hyperfine interaction can be resolved. For this direction an effective  $K^{Cd} = 17 \times 10^{-4} \text{ cm}^{-1}$  value is determined. In the lower part of Fig. 2 the calculated EPR spectrum using Eq. (1) and the parameters determined is shown. The close similarity between the experimental and calcu-

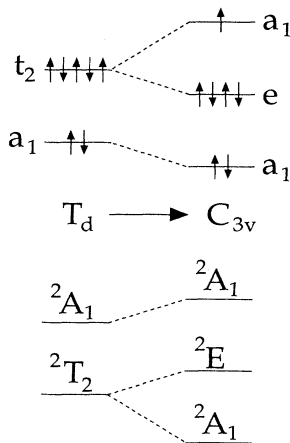


FIG. 1. Schematic energy-level diagram for the  $V_{Cd}^-$  center using the single-particle states (top) and many-electron states (bottom).

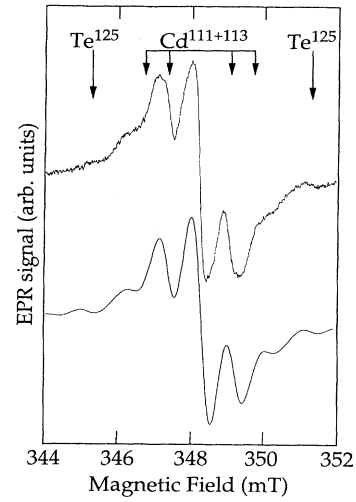


FIG. 2. Experimental (top) and calculated (bottom) EPR spectra of  $V_{Cd}^-$ . The hyperfine splittings caused by  $Te^{125}$  and by  $Cd^{111}$  and  $Cd^{113}$  are indicated.

lated spectra is a strong argument in favor of the interpretation that the EPR spectrum corresponds to the isolated cadmium vacancy. The fact that "single Te atom" hyperfine splitting is much stronger than the Cd hyperfine one, and that no hyperfine structure from the other three Te neighbors of the Cd vacancy is observed, supports the model of the unpaired electron localized on one Te atom.

The EPR signal from the singly negatively charged  $V_{\text{Cd}}^-$  center is strongest when the sample is not illuminated. When illuminated with the light of photon energy ( $h\nu$ ) equal to or larger than 0.47 eV, a slight decrease is observed, but if  $h\nu$  is larger than the band gap ( $E_g$ ) the decrease of the EPR intensity is smaller. Since the material is *p* type, the energy levels cannot communicate with the conduction band as long as  $h\nu < E_g/2$ . We interpret the decrease of the EPR intensity as a hole being emitted from the  $2-/-$  level of  $V_{\text{Cd}}^-$  to the valence band. When  $h\nu > E_g$ , electron-hole pairs are created and  $V_{\text{Cd}}^{2-}$  centers can recapture a hole and thus contribute to the EPR signal. These experiments therefore indicate that the  $2-/-$  level of  $V_{\text{Cd}}^-$  is positioned at  $E_v + 0.47$  eV. However, since the  $V_{\text{Cd}}^-$  center is Jahn-Teller distorted, care must be taken when analyzing these data. A configurational coordinate diagram for the  $V_{\text{Cd}}^-$  center is shown in Fig. 3. In this figure,  $Q$  is the distortion coordinate for the trigonal Jahn-Teller relaxation of  $V_{\text{Cd}}^-$ . The lower curve represents the total energy of  $V_{\text{Cd}}^-$ , which has a minimum when the defect is distorted. The upper curve, which is displaced upwards with  $E_g$  compared to the lower one, gives the total energy for  $V_{\text{Cd}}^-$  plus an electron-hole pair. The third curve, finally, shows the total energy for  $V_{\text{Cd}}^{2-}$  plus a free hole in the valence band, and this curve has a minimum at the undistorted site ( $T_d$  symmetry). Also, the vertical optical transition corresponding to the ionization in the photo-EPR experiment is indicated in the figure. As can be seen, this photon energy does not correspond to the distance between the  $2-/-$  level and the valence band, but instead to this distance plus  $E_{\text{JT}}$  (the Jahn-Teller energy). It is therefore not possible to determine the level position only from these photo-EPR measurements. We can only say that the level is closer than 0.47 eV to the valence band.

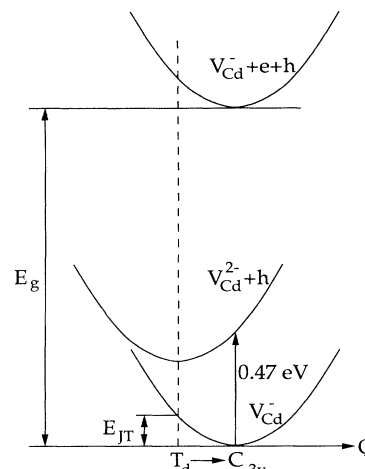


FIG. 3. Configuration coordinate diagram for the cadmium vacancy. For details, see text.

#### IV. CONCLUSIONS

In conclusion, we have reported the EPR spectrum of the isolated cadmium vacancy in CdTe. The defect is detected in its single negative charge state and the symmetry is found to be trigonal. In the proposed model the hole occupies a  $t_2$  orbital of the dangling bonds of the tellurium neighbors, and the orbital degeneracy is removed by a trigonal Jahn-Teller distortion. The hyperfine interaction shows that the hole is localized on one of the Te atoms. From photo-EPR experiments it is shown that the  $2-/-$  level of the Cd vacancy is positioned less than 0.47 eV above the valence band.

#### ACKNOWLEDGMENTS

The authors are grateful to Professor Dr. P. Rüdolph for providing the crystals. This work was supported by the Swedish Natural Science Research Council and by the Swedish Board for Industrial and Technical Development.

<sup>1</sup>A. Herve and B. Maffeo, Phys. Lett. **32A**, 247 (1970).

<sup>2</sup>D. Galland and A. Herve, Phys. Lett. **33A**, 1 (1970).

<sup>3</sup>G. D. Watkins, Air Force Research Laboratory, Technical Report No. ARL TR75-0011, 1975 (unpublished), available from the National Technical Information Service, Clearinghouse, Springfield, VA 22151.

<sup>4</sup>Y. Shono, J. Phys. Soc. Jpn. **47**, 590 (1979).

<sup>5</sup>G. D. Watkins, Bull. Am. Phys. Soc. **14**, 312 (1969).

<sup>6</sup>A. L. Taylor, G. Filipovich, and G. K. Lindeberg, Solid State Commun. **9**, 945 (1971).

<sup>7</sup>K. M. Lee, Le Si Dang, and G. D. Watkins, Solid State Commun. **35**, 527 (1980).

<sup>8</sup>K. M. Lee, Le Si Dang, and G. D. Watkins, in *Defects and Radiation Effects in Semiconductors 1980*, edited by R. R. Hasiguti, IOP Conf. Proc. No. 59 (Institute of Physics, Bristol and

London, 1981), p. 353.

<sup>9</sup>K. M. Lee, K. P. O'Donnell, and G. D. Watkins, Solid State Commun. **41**, 881 (1982).

<sup>10</sup>G. Brunthaler, W. Jantsch, U. Kaufmann, and J. Schneider, J. Phys. Condens. Matter **1**, 1925 (1989).

<sup>11</sup>D. M. Hofmann, P. Omling, H. G. Grimmeiss, B. K. Meyer, K. W. Benz, and D. Sinerius, Phys. Rev. B **45**, 6247 (1992).

<sup>12</sup>W. Stadler, D. M. Hofmann, B. K. Meyer, B. Kowalski, P. Emanuelsson, P. Omling, E. Weigel, and G. Müller-Vogt (unpublished).

<sup>13</sup>B. K. Meyer, P. Omling, E. Weigel, and G. Müller-Vogt, Phys. Rev. B **46**, 15 135 (1992).

<sup>14</sup>M. Winecke, H. Berger, and M. Schenk, Mater. Sci. Eng. B (to be published).